BIOCHEMISTRY
including biophysical chemistry & molecular biology
Article

Biochemistry **2011,** *50,* 329–339 329
DOI: 10.1021/bi101077e

S4 Protein Sll1252 Is Necessary for Energy Balancing in Photosynthetic Electron Transport in *Synechocystis* sp. PCC 6803[†]

Natsuko Inoue-Kashino,[‡,§,∥] Yasuhiro Kashino,[*,‡,§] Hidefumi Orii,[§] Kazuhiko Satoh,[§] Ichiro Terashima,[∥,⊥] and Himadri B. Pakrasi[‡]

[‡]*Department of Biology, Washington University, St. Louis, Missouri 63130, United States,* [§]*Department of Life Science, Graduate School of Life Science, University of Hyogo, Ako-gun, Hyogo 678-1297, Japan, and* [∥]*Department of Biology, Graduate School of Science, Osaka University, Toyonaka, Osaka 560-0043, Japan.* [⊥]*Current address: Department of Biological Sciences, The University of Tokyo, Bunkyo-ku, Tokyo 113-0033, Japan.*

Received July 6, 2010; Revised Manuscript Received November 25, 2010

ABSTRACT: Sll1252 was identified as a novel protein in photosystem II complexes from *Synechocystis* sp. PCC 6803. To investigate the function of Sll1252, the corresponding gene, *sll1252*, was deleted in *Synechocystis* 6803. Despite the homology of Sll1252 to YlmH, which functions in the cell division machinery in *Streptococcus*, the growth rate and cell morphology of the mutant were not affected in normal growth medium. Instead, it seems that cells lacking this polypeptide have increased sensitivity to Cl^- depletion. The growth and oxygen evolving activity of the mutant cells was highly suppressed compared with those of wild-type cells when Cl^- and/or Ca^{2+} was depleted from the medium. Recovery of photosystem II from photoinhibition was suppressed in the mutant. Despite the defects in photosystem II, in the light, the acceptor side of photosystem II was more reduced and the donor side of photosystem I was more oxidized compared with wild-type cells, suggesting that functional impairments were also present in cytochrome b_6/f complexes. The amounts of cytochrome c_{550} and cytochrome *f* were smaller in the mutant in the Ca^{2+}- and Cl^--depleted medium. Furthermore, the amount of IsiA protein was increased in the mutant, especially in the Cl^--depleted medium, indicating that the mutant cells perceive environmental stress to be greater than it is. The amount of accompanying cytochrome c_{550} in purified photosystem II complexes was also smaller in the mutant. Overall, the Sll1252 protein appears to be closely related to redox sensing of the plastoquinone pool to balance the photosynthetic electron flow and the ability to cope with global environmental stresses.

Photosystem (PS)[1] II is a multisubunit membrane protein complex that mediates photocatalytic water oxidation to yield molecular oxygen (*1*−*4*). The 20 subunit proteins are assembled stoichiometrically into a single complex to form a functional PS II complex, as shown by crystallographic models obtained from two strains of cyanobacteria, *Thermosynechococcus elongatus* (*1*, *2*, *4*) and *Thermosynechococcus vulcanus* (*3*). In addition to the assembled subunit proteins, several proteins were found to be associated with highly purified PS II core complexes from a cyanobacterium, *Synechocystis* sp. PCC 6803, by proteomic analyses (*5*). These proteins included five novel proteins whose functions were unknown: Sll1130, Sll1252, Sll1390, Sll1414, and Sll1638. One of these proteins, Sll1638, was found to be homologous to plant PsbQ protein (17 kDa protein) (*5*). It was subsequently proven that Sll1638 associated stoichiometrically with the lumenal side of PS II and played an important role in water oxidation in PS II (*6*, *7*). Auxiliary functions to support the assembly and repair of PS II complexes have been shown for Sll1414 (Psb29) and TLP18.3 protein, a homologue of Sll1390 in *Arabidopsis thaliana* (*8*, *9*), as found in Psb27 (*10*−*12*).

Among the five novel proteins mentioned above, the function of Sll1252 has not yet been characterized. It has been proposed that Sll1252 has a particularly unique characteristic, because it has been predicted that Sll1252 contains an S4 domain (*13*). An S4 domain is a small domain consisting of 60−65 amino acid residues that is predicted to mediate binding to RNA (*14*). Although a number of small proteins are recognized to have an S4 domain, many of them have not been characterized but are assumed to be involved in translational regulation (*14*). YlmH (*15*), a protein that acts in cell division in a Gram-positive bacterium, *Streptococcus pneumoniae*, is also included in the same Pfam (*16*) protein family, *S4*, and is highly homologous to *sll1252* in *Synechocystis* 6803 and the corresponding *orf1324* in *Synechococcus* sp. PCC 7942 (*17*), although cyanobacteria are Gram-negative in morphology (*18*). The corresponding gene is also conserved in *Arabidopsis* (At1g53120) (*5*). It has been suggested that these YlmH

[†]This work was supported by the Ministry of Education, Culture, Sports, Science and Technology, Japan (18054028 and 18GS0318 to Y.K.), grants from Hyogo Prefecture (Y.K.) and the Hyogo Science and Technology Association (Y.K.), Sasakawa Scientific Research Grants from The Japan Science Society (21-417 to N.I.-K.), and the National Science Foundation (MCB0745611 to H.B.P.).

*To whom correspondence should be addressed: Department of Life Science, Graduate School of Life Science, University of Hyogo, 3-2-1 Koto, Kamigori, Ako-gun, Hyogo 678-1297, Japan. Phone and fax: +81-791-58-0185. E-mail: kashino@sci.u-hyogo.ac.jp.

[1]Abbreviations: α, initial slope in the light curve; Chl, chlorophyll; CP47, peripheral Chl-binding proteins of 47 kDa of photosystem II; cyt, cytochrome; DCBQ, dichloro-*p*-benzoquinone; DCIP, 2,6-dichlorophenolindophenol; DCMU, 3-(3,4-dichlorophenyl)-1,1-dimethylurea; F and F'_m, transient and maximal fluorescence levels at a given time under actinic light, respectively; F'_o, minimal fluorescence level after far-red light illumination; F_m and F_v, maximal and variable fluorescence yields, respectively; I_k, intensity at which light saturation is attained; Km^r and Gm^r, kanamycin and gentamycin resistance cartridges, respectively; PS, photosystem; MES, 2-(*N*-morpholino)ethanesulfonic acid; P_{max}, maximal photosynthetic rate; PCR, polymerase chain reaction; SDS−PAGE, sodium dodecyl sulfate−polyacrylamide gel electrophoresis.

© 2010 American Chemical Society
Published on Web 12/08/2010

homologues play roles in cell division in cyanobacteria and plastid division in eukaryotes (*17*). However, *ylmH* was not included among the various genes that caused filamentous morphologies by transposon insertions in *Synechococcus* 7942 (*17*), suggesting a different function of YlmH in cyanobacteria.

The corresponding gene in higher plants such as *Arabidopsis* (At1g53120) and rice (Os01g0747700) is encoded in the nuclear genome. The gene product has an N-terminal extension, and TargetP (*19*) predicts that it may be delivered to mitochondria. Recently, the gene product was detected in chloroplasts (*20*). Judging from the association of the Sll1252 protein with PS II core complexes and the presence of the corresponding protein in higher plant chloroplasts, it is highly possible that Sll1252 may have functions differing from that in cell division. In this study, we deleted the *sll1252* gene from *Synechocystis* 6803 and found that Sll1252 was important for the normal function of photosynthetic electron transport by achieving an overall redox balance.

EXPERIMENTAL PROCEDURES

Cyanobacterial Strains and Growth Conditions. *Synechocystis* 6803 cells (wild-type cells and mutant cells lacking Sll1252) were grown as described previously (*21*) in BG11 medium (*22*).

Ca^{2+}- and/or Cl^--depleted BG11 medium was prepared in plasticware to exclude contamination by ions as described previously (*21*). Fe-depleted BG11 medium was prepared using sodium ammonium citrate instead of ferric ammonium citrate. Growth was monitored by measuring the optical density at 730 nm (OD_{730}) in an MQX200 μQuant Universal Microplate Spectrophotometer as described previously (*21*).

Gene Cloning and Isolation of Mutants. Deletion of the *sll1252* gene was conducted using a previously described strategy (*21*) with two pairs of PCR primers for cloning: primers P1 (5′-TACTAAAGCCAGCACACTCA-3′) and P2 (5′-CGAGCA-ACGGCATTAGCTAA-3′) for region 1738717−1738118 in the genome of *Synechocystis* 6803 [CyanoBase (*23*)], and primers P3 [5′-GCGCGGAGCTCGATGATATCTTTTGCCAGTG-3′ (a *Sac*I restriction site is underlined)] and P4 [5′-GCGCG-GAGCTCGTTTGGGTAAAGGTCAAACT-3′ (a *Sac*I restriction site is underlined)] for region 1737317−1736738. The resulting plasmid construct with a gentamycin resistance cartridge (Gm^r) (*24*) was used to delete the *sll1252* gene from the wild-type and HT3 (Km^r) strains of *Synechocystis* 6803. The HT3 strain (*25*), which has a hexahistidine tag at the carboxyl terminus of CP47 and carries a kanamycin resistance cartridge (Km^r) (*26*), was a generous gift from T. M. Bricker (Louisiana State University, Baton Rouge, LA).

To introduce a hexahistidine tag at the C-terminus of Sll1252, a plasmid construct carrying a Km^r cartridge was created as described previously (*27*). The following two pairs of PCR primers were used for cloning: primers 5 (5′-GTCATCGCCGGGGTTT-GAAG-3′) and 6 [5′-TTAGTGGTGATGGTGATGGTGAA-GATATCGGGTTAATTGG-3′ (the sequence corresponding to the hexahistidine tag is underlined)] for region 1738239−1737341 in the *Synechocystis* 6803 genome, and primers 7 [5′-GCGCG-GTCGACCCAGTTTCAAGGCTTGCC-3′ (a *Sal*I restriction site is underlined)] and 8 [5′-GCGCGGAGCTCCCGGCACA-AAATTTTCCG-3′ (a *Sac*I restriction site is underlined)] for region 1737337−1736538.

The accuracy of the sequences of the PCR products was checked by sequencing, and complete segregation of the mutations was confirmed by PCR (data not shown).

Isolation of Thylakoid Membranes and PSII Complexes. Thylakoid membranes from the wild-type and ΔSll1252 strains and PS II complexes from the HT3 and ΔSll1252/HT3 strains were isolated as previously described (*5*, *21*).

Electrophoresis and Polypeptide Detection. SDS−PAGE was performed using 18 to 24% gradient acrylamide gels containing 6 M urea or gels containing 16% acrylamide and 6 M urea (*28*, *29*). Antisera against PsaA/B (CP1-e), PsbC (CP43), PsbO (*30*), cytochrome c_{550} (*31*), IsiA (AgriSera, Vännäs, Sweden), and polyhistidine (Sigma, St. Louis, MO) were used for immunodetection. Heme was detected by chemiluminescence using West-Femto reagents (Pierce, Rockford, IL) after electroblotting (*28*).

Oxygen Evolution Assays. Cells cultured for 3 days in normal or Ca^{2+}- and/or Cl^--depleted BG11 medium were washed, resuspended in the respective fresh BG11 medium at a concentration of 10 μg of chlorophyll (Chl)/mL, and used for assays of PS II-mediated activity in whole cells. The Chl concentration was determined by the method of Porra et al. (*32*). Steady-state oxygen evolution was measured with a Clark-type electrode in the presence of 0.5 mM 2,6-dichloro-*p*-benzoquinone (DCBQ) as an electron acceptor as described previously (*21*). The photosynthetic rate was plotted versus light intensity, and the photosynthetic parameters were obtained by fitting the curve (*33*) using the data analysis software KaleidaGraph version 3.6 (Synergy Software, Reading, PA). The oxygen flash yield measured on a bare platinum electrode (Artisan Scientific Co., Urbana, IL) and the S-state distribution and parameters were calculated as described previously (*21*).

Fluorescence Kinetics. Fluorescence decay kinetics were measured using an FL-3200 double-modulation fluorometer (Photon System Instruments, Brno, Czech Republic) with a built-in analysis program, FluorWin, at room temperature (*6*, *34*).

The fluorescence kinetics were also measured using a conventional method in a PAM 101 pulse amplitude modulation fluorometer (Walz GmbH, Effeltrich, Germany) (*21*) to assess the reduction level of Q_A in the cells. A saturating light pulse was applied every 30 s under actinic light for ~4.5 min, followed by far-red light for 1 min and a succeeding 2 min period without illumination. On the basis of these measurements, the reduction level of Q_A was calculated using the values at the end of the actinic light and the term $(F - F'_o)/(F'_m - F'_o)$, where F and F'_m are the transient and maximal fluorescence levels at a given time under the actinic light, respectively, and F'_o is the minimal fluorescence level after far-red light illumination.

Light-Induced Oxidation−Reduction Kinetics of P700. Light-induced redox changes of P700 were monitored at 810 nm with a reference wavelength of 870 nm using the PAM101 fluorometer equipped with a dual-wavelength P700 unit (ED-P700DW, Walz). The kinetics data were fitted to exponential curves using KaleidaGraph with a Levenberg−Marquardt regression algorithm.

Photoinhibition Measurement. Photoinhibition measurements were performed as described previously (*21*) using cells that had been cultured for 2 days, washed, and resuspended in fresh normal BG11 medium at a concentration of 2 μg of Chl/mL.

State Transition Experiments. State transition occurred in cells grown in normal BG11 medium as described previously (*35*).

Spectroscopic Measurements. Fluorescence emission spectra at 77 K were recorded using a Fluoromax-2 fluorometer (Jobin Yvon, Cedex, France) as described previously (*5*). The cytochrome (cyt) b_{559} content was estimated as described previously (*5*).

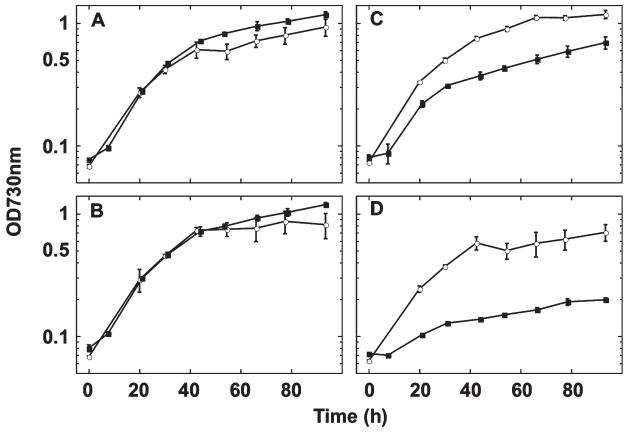

FIGURE 1: Effects of Ca^{2+} and/or Cl^- on cyanobacterial growth. (A−D) Cells were cultured in normal BG11 medium for 3 days, washed three times, and resuspended in Ca^{2+}- and Cl^--depleted BG11 medium. The cells were then diluted to an OD_{730} of 0.06−0.07 with normal (A), Ca^{2+}-depleted (B), Cl^--depleted (C), or Ca^{2+}- and Cl^--depleted (D) BG11 medium. The cells were grown on a rotary shaker at 30 °C under 50 μmol of photons m^{-2} s^{-1} for each medium condition: (○) wild-type cells and (■) ΔSll1252. Error bars show the standard deviation (SD) (n = 3). The Cl^- concentrations in Cl^--depleted BG11 medium and Ca^{2+}- and Cl^--depleted BG11 medium were below the detectable limit (< 20 μM).

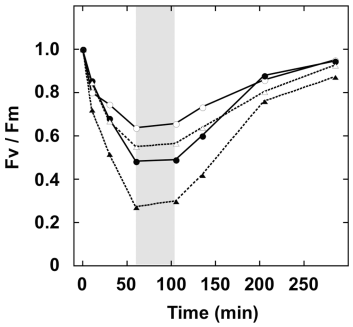

FIGURE 2: Assessment of sensitivity to photoinhibition. Cells (2 μg of Chl/mL) were exposed to 900 μmol of photons m^{-2} s^{-1} at 30 °C in the absence (empty symbols) or presence (filled symbols) of chloramphenicol (100 μg/mL), and the F_v/F_m ratio was measured. After a 60 min exposure to high level of light, the cells were washed twice to remove the chloramphenicol and then incubated under 20 μmol of photons m^{-2} s^{-1} at 30 °C. The duration of the washing is shown by the shaded bar: (circles) wild-type cells and (triangles) ΔSll1252 cells. The values were normalized by the initial values.

RESULTS

Protein Profile Assessed with Gene Information. The deduced amino acid sequence of Sll1252 was obtained from CyanoBase (*23*). The length is 259 amino acids; the predicted molecular weight is 28591, and the theoretical pI is 7.82. It was predicted to be a soluble protein by hydropathy plotting (*36*), the SOSUI program (*37*), and the ExPASy ProtParam tool (*38*). A transit peptide was not predicted by LipoP (*39*) or ChloroP (*40*). Accordingly, the Sll1252 protein is expected to function in the stromal space of cells.

An S4 domain resides in the C-terminal region of Sll1252 (amino acids 184−230). Another S4 protein is present in *Synechocystis* 6803: Slr0469 or 30S ribosomal protein S4. The phylogenetic relationship among proteins with S4 domains is shown in Figure S1 of the Supporting Information. The proteins homologous to Sll1252, including those in *Arabidopsis* and rice, form a group that is clearly separated from the other group of S4 proteins in photosynthetic organisms and other proteins with S4 domains in bacteria.

Expression of Sll1252 in Cells. The accumulation of Sll1252 was assessed using two mutants expressing histidine-tagged Sll1252 and histidine-tagged CP47. However, the anti-His antibody could not detect the histidine-tagged Sll1252 using a cell equivalent to 10 μg of Chl on the electrophoresis gel (data not shown).

Effects of the Gene Deletion on Growth. The shape and size of the *sll1252* deletion mutant cells (termed ΔSll1252 cells hereafter) were not distinguishable from those of wild-type cells under microscopic observation (data not shown). The growth rates of the wild-type and mutant cells were examined under normal and Ca^{2+}- and/or Cl^--depleted conditions. In normal BG11 medium, wild-type and ΔSll1252 cells grew similarly, showing logarithmic growth during the initial ~20 h and then entering a stationary phase (Figure 1A). In the Ca^{2+}-depleted medium (Figure 1B), the growth rates of wild-type and ΔSll1252 cells did not differ remarkably. Upon depletion of Cl^- from the growth medium, the growth rate of ΔSll1252 cells was markedly suppressed compared with that of wild-type cells (Figure 1C). When both Ca^{2+} and Cl^- were depleted (Figure 1D), the growth rate of ΔSll1252 cells was drastically suppressed.

The effect of nutrient depletion on the growth was in good accordance with the effect on the oxygen-evolving process in cells measured in the presence of 0.5 mM 2,5-DCBQ as an electron acceptor (Figure S2 and Table S1 of the Supporting Information). When the cells were grown in normal BG11 medium, the efficiency of light utilization (α), the apparent maximum value of activity (P_{max}), and the light intensity at which the photosynthesis began to become saturated (I_k) in ΔSll1252 cells were approximately the same as those in wild-type cells. These findings indicate that PS II functioned almost normally in ΔSll1252 cells when they were grown in normal BG11 medium. When both Ca^{2+} and Cl^- were limited in the growth medium, all of these photosynthetic parameters were decreased in both wild-type and ΔSll1252 cells. Furthermore, the effects appeared to be more severe in ΔSll1252 cells, because the α value in ΔSll1252 cells was 33% of the value in wild-type cells and P_{max} was 54% of the value in wild-type cells. These findings imply that the oxygen-evolving machinery was highly impaired or the level of active PS II was greatly decreased in ΔSll1252 cells when Ca^{2+} and Cl^- were limited.

The functional liability of the donor side of PS II in the cells when both Ca^{2+} and Cl^- were limited in the growth medium was also supported by the oxygen flash yield (Table S2 of the Supporting Information). The probability of a mishit was almost the same in all cells. The probability of a double hit in ΔSll1252 cells grown under the Ca^{2+}- and Cl^--limited condition was higher than that in wild-type cells. The most prominent modification was observed in the ratio of S1 to S0 in ΔSll1252 cells grown in the Ca^{2+}- and Cl^--depleted medium.

Sensitivity to Photoinhibition in Cells. When the cells were exposed to a high level of light (900 μmol of photons m^{-2} s^{-1}), the PS II activity in cells determined as the F_v/F_m ratio decreased somewhat faster in ΔSll1252 cells than in wild-type cells in the absence of chloramphenicol (Figure 2). Under the subsequent low-light condition (20 μmol of photons m^{-2} s^{-1}), the PS II activity recovered to the initial level within 3 h in both strains. In the presence of chloramphenicol (Figure 2), the PS II activity in wild-type cells under a high level of light decreased to the same extent as that in ΔSll1252 cells without chloramphenicol treatment. Under this light intensity, ΔSll1252 cells were quite susceptible to photoinhibition when chloramphenicol was present, indicating

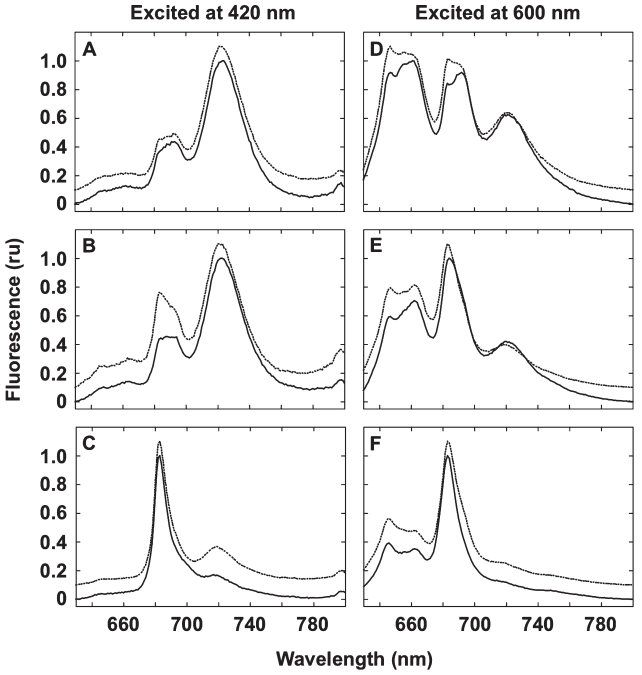

FIGURE 3: Fluorescence emission spectra of cyanobacterial cells at 77 K (A and D) grown in normal BG11 medium, (B and E) grown in Cl^--depleted medium, and (C and F) grown in Fe-depleted medium. The chromophores were excited at 77 K and 420 (A−C) or 600 nm (D−F). The fluorescence signals were normalized at the highest peak. The spectra were offset for the sake of clarity: (—) wild-type cells and (···) ΔSll1252 cells.

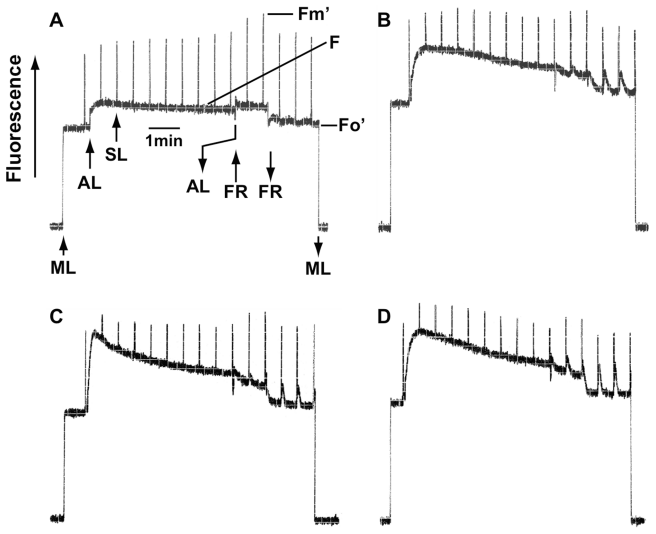

FIGURE 4: Light-induced fluorescence kinetics in cyanobacterial cells. (A−D) Fluorescence yields were recorded in wild-type (A and B) and ΔSll1252 (C and D) cells grown in normal (A and C) or Cl^--depleted (B and D) BG11 medium at a concentration of 4 μg of Chl/mL. Abbreviations: ML, measuring light; AL, actinic light; SL, saturating light; FR, far-red light; F, fluorescence yield under the actinic light; Fo′, fluorescence yield under the far-red light; Fm′, fluorescence yield upon a saturating flash. Typical traces are shown.

that PS II complexes were unstable without Sll1252. After the removal of chloramphenicol, the PS II activity promptly recovered, showing that the biosynthesis system for PS II was almost normal.

Effects of the Absence of Sll1252 on the Energy Distribution in the Cells. The energy distribution among PS I, PS II, and antenna proteins was assessed by measuring the fluorescence spectra at 77 K in the cells (Figure 3). In cells grown in normal BG11 medium and excited at a wavelength of 420 nm, which preferentially excites Chl molecules, the relative ratio of PS II fluorescence (685 and 695 nm) to PS I fluorescence (720 nm) was slightly lower in ΔSll1252 cells than in wild-type cells, and a small but distinct increase was observed at 680 nm in the mutant cells (Figure 3A). When Cl^- was depleted in the growth medium, the relative ratio of PS II to PS I was increased in both wild-type and ΔSll1252 cells (Figure 3B). In addition, the fluorescence at 680 nm increased slightly in wild-type cells and remarkably in the mutant cells. The wavelength was shorter than the ordinary fluorescence from PS II (e.g., ref *5*) and very close to that from IsiA, which is induced under iron-deficient conditions (*41*, *42*). To verify the identity of the shorter wavelength fluorescence, the cells were grown under iron-depleted conditions and the fluorescence spectra were obtained (Figure 3C). In both wild-type and Sll1252 cells, fluorescence was observed almost entirely at 681 nm, which is identical to the wavelength increase in Figure 3B, thereby confirming that the level of IsiA was increased in Sll1252 cells especially under the Cl^--depleted condition (see also Figure 9).

Similar profiles were found when the cells were illuminated at 600 nm to preferentially excite phycobilisome (Figure 3D−F). The relative content of phycobilisome decreased when both wild-type and ΔSll1252 cells were grown in the Cl^--depleted medium (Figure 3E).

Redox Level of the Electron Transport Chain during Light Illumination. The increase in the level of IsiA in ΔSll1252 cells (Figure 3) also suggests oxidative stress (*42*). Therefore, we assessed the redox level of the electron transport chain under light by measuring the fluorescence kinetics under continuous illumination and in the postillumination periods in cells grown in normal or Cl^--depleted BG11 medium (Figure 4).

Wild-type cells grown in normal BG11 medium exhibited typical kinetics (Figure 4A). When wild-type cells were grown in the Cl^--depleted medium, the photochemical quenching $[(F'_m - F)/(F'_m - F'_o)]$ appeared to become smaller (Figure 4B), showing greater reduction of Q_A. The transient increase in fluorescence that follows F'_m in the dark (after the light has been turned off) also indicated greater reduction of the plastoquinone pool (Figure 4B).

The photochemical quenching under light and the transient increase in fluorescence in the dark in ΔSll1252 cells grown in normal BG11 medium (Figure 4C) were similar to those in wild-type cells grown in the Cl^--depleted medium (Figure 4B). When ΔSll1252 cells were grown in the Cl^--depleted medium, the extent of photochemical quenching was further decreased (Figure 4D). Furthermore, the reoxidation rate after a saturating pulse was drastically decreased under the far-red light (Figure 4D) compared with that of wild-type cells, indicating a remarkable reduction of plastoquinone. A decreased rate of reoxidation of Q_A^- was also observed in ΔSll1252 cells grown in normal BG11 medium, although the extent was not so remarkable.

The reducing levels were quantitatively evaluated for wild-type and ΔSll1252 cells grown in normal or Ca^{2+}- and/or Cl^--depleted BG11 medium (Table 1). It was evident that, even when the cells were grown in normal BG11 medium, the reduction level of Q_A was increased remarkably in ΔSll1252 cells. Upon depletion of Cl^- from the growth medium, Q_A was further reduced in ΔSll1252 cells. Interestingly, increases in the reducing levels of Q_A were observed in wild-type cells when they were grown in the Cl^--depleted medium, although the increases were inferior to those in the corresponding ΔSll1252 cells. The progressive reduction in the level of plastoquinone could perturb the state transition.

Table 1: Reduction Levels of Q_A $[(F'_m - F)/(F'_m - F'_o)]$ during Light Illumination[a]

strain	BG11	without Ca^{2+}	without Cl^-	without Ca^{2+} and Cl^-
wild-type	0.139 ± 0.014	0.102 ± 0.0018	0.333 ± 0.029	0.306 ± 0.011
ΔSll1252	0.390 ± 0.0094	0.350 ± 0.0000	0.418 ± 0.016	0.528 ± 0.016

[a]Wild-type and ΔSll1252 cells grown in normal, Ca^{2+}-depleted, Cl^--depleted, or Ca^{2+}- and Cl^--depleted BG11 medium were evaluated. The reduction levels of Q_A $[(F'_m - F)/(F'_m - F'_o)]$ were calculated using the values at the end of actinic light illumination as shown in Figure 4. Standard errors are given ($n = 3$).

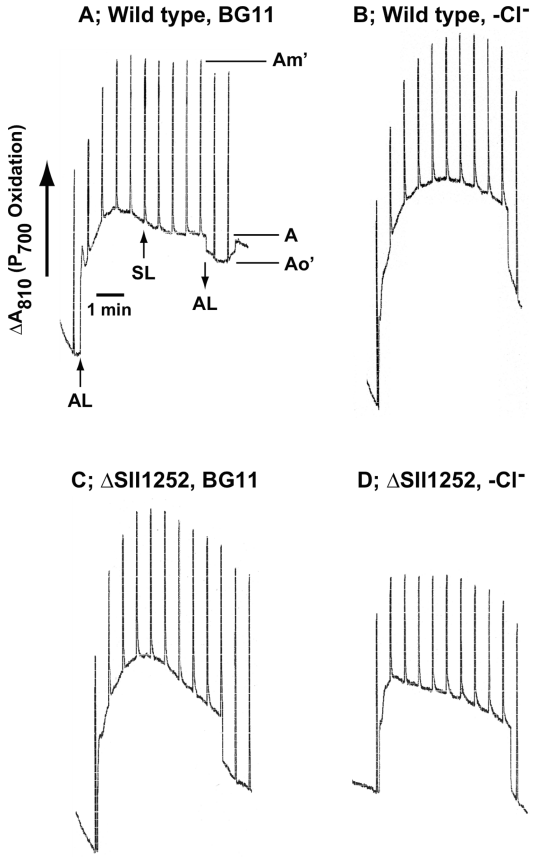

FIGURE 5: Light-induced oxidation−reduction kinetics of P700. (A−D) Wild-type (A and B) and ΔSll1252 (C and D) cells were grown in normal (A and C) or Cl^--depleted (B and D) BG11 medium. The absorbance changes of P700 were recorded at 810 nm using a PAM101 fluorometer equipped with a dual-wavelength P700 unit (ED-P700DW). The Chl concentration was 4 μg/mL. Actinic light (AL) was turned on and off at the times indicated by the arrows (upward, turn on; downward, turn off). Abbreviations: SL, saturating light; A, absorbance level under the actinic light; Ao, absorbance level in the dark; Am′, absorbance level after a saturating flash. Typical traces are shown.

The fluorescence spectra at 77 K measured at state I (Figure S3 of the Supporting Information, solid line) were almost identical between wild-type and ΔSll1252 cells. In contrast, the fluorescence spectra at 77 K differed between the two strains under the state II condition. Specifically, the relative ratio of PS I to PS II was much more greatly increased in ΔSll1252 cells than in wild-type cells, indicating a higher reduction level of the plastoquinone pool.

Because the reducing level of the plastoquinone pool was increased in the mutant cells, the reduction level of P700 during light illumination was assessed (Figure 5 and Table 2). The reducing levels of P700 were smaller in ΔSll1252 cells than in wild-type cells, even when they were grown in normal BG11 medium (Table 2). Upon depletion of Cl^-, and also Ca^{2+}, the reducing levels of P700 during light illumination were further decreased in ΔSll1252 cells. Taken together, the data shown in Figures 4 and 5 and Tables 1 and 2 indicate decelerated electron flow between Q_A and P700. To determine the site of the defects in the electron flow more precisely, the kinetics of the oxidation and reduction of P700 were measured under three different conditions.

Activity of Cyclic Electron Flow. The involvement of the cyclic electron flow around PS I was investigated by measuring the oxidation−reduction kinetics of P700 in the presence of DCMU (Figure 6 and Table 3). The oxidation kinetics upon light illumination were almost identical between wild-type and ΔSll1252 cells, irrespective of the growth conditions. The rates of re-reduction of P700 via cyclic electron flow after the light had been turned off were slower in ΔSll1252 cells by up to 20% compared with the rates in wild-type cells, except when the cells were grown in the Ca^{2+}-depleted medium.

Rates of Donation of Electrons to P700 via Plastocyanin/Cytochrome c_6. The rates of donation of electrons from plastocyanin/cytochrome c_6 (*43*) were assessed by measuring the oxidation−reduction kinetics of P700 in the presence of 50 μM DCMU as a PS II inhibitor and 5 mM ascorbate and 0.5 mM DCIP as electron donors to plastocyanin/cytochrome c_6 (Figure 7 and Table 3). The rates of oxidation upon illumination and re-reduction during subsequent darkness for P700 were identical between the two strains when the cells were grown under the same conditions, confirming that there was no remarkable impairment of the electron flow from plastocyanin/cytochrome c_6 to P700. The inconsistency between the measured and fitted decay curves at the beginning of P700 re-reduction in Cl^--depleted cells (Figure 7C,D) was quite similar between wild-type and ΔSll1252 cells.

Rates of Donation of Electrons to P700 via Cytochrome b_6/f. The electron flow through cytochrome b_6/f complexes was assessed by measuring the oxidation−reduction kinetics of P700 in the presence of 50 μM DCMU as a PS II inhibitor and 10 mM ascorbate and 1 mM duroquinone as electron donors to cytochrome b_6/f complexes (Figure 8 and Table 3). The kinetics of P700 re-reduction via cytochrome b_6/f was not correctly fitted to one-exponential decay curves (Figure 8), implying additional (minor) electron flow to P700. However, it is evident that the rate of re-reduction of P700 in the dark was clearly decelerated in ΔSll1252 cells, irrespective of the growth conditions. Because of the slower re-reduction rate of P700 in ΔSll1252 cells, the oxidation rate of P700 in the mutant cells was faster than that in wild-type cells (Figure 8). These results confirm that there were functional defects in cytochrome b_6/f complexes because no detectable defects were observed in the electron flow from plastocyanin/cytochrome c_6 to P700 (Figure 7 and Table 3).

Polypeptide Composition. To address the defects in PS II and cytochrome b_6/f complexes, the amounts of polypeptides on PS I, PS II, and cytochrome b_6/f complexes were evaluated after

Table 2: Reduction Levels of P700 $[(A'_m - A)/(A'_m - A_o)]$ during Light Illuminatio[a]n

strain	BG11	without Ca^{2+}	without Cl^-	without Ca^{2+} and Cl^-
wild-type	0.926 ± 0.0058	0.839 ± 0.0092	0.744 ± 0.0013	0.708 ± 0.016
ΔSll1252	0.790 ± 0.0060	0.714 ± 0.0042	0.664 ± 0.015	0.645 ± 0.0095

[a]Wild-type and ΔSll1252 cells grown in normal, Ca^{2+}-depleted, Cl^--depleted, or Ca^{2+}- and Cl^--depleted BG11 medium were evaluated. The reduction levels of P700 $[(A'_m - A)/(A'_m - A_o)]$ were calculated using the values at the end of actinic light illumination as shown in Figure 5. Standard errors are given ($n = 3$).

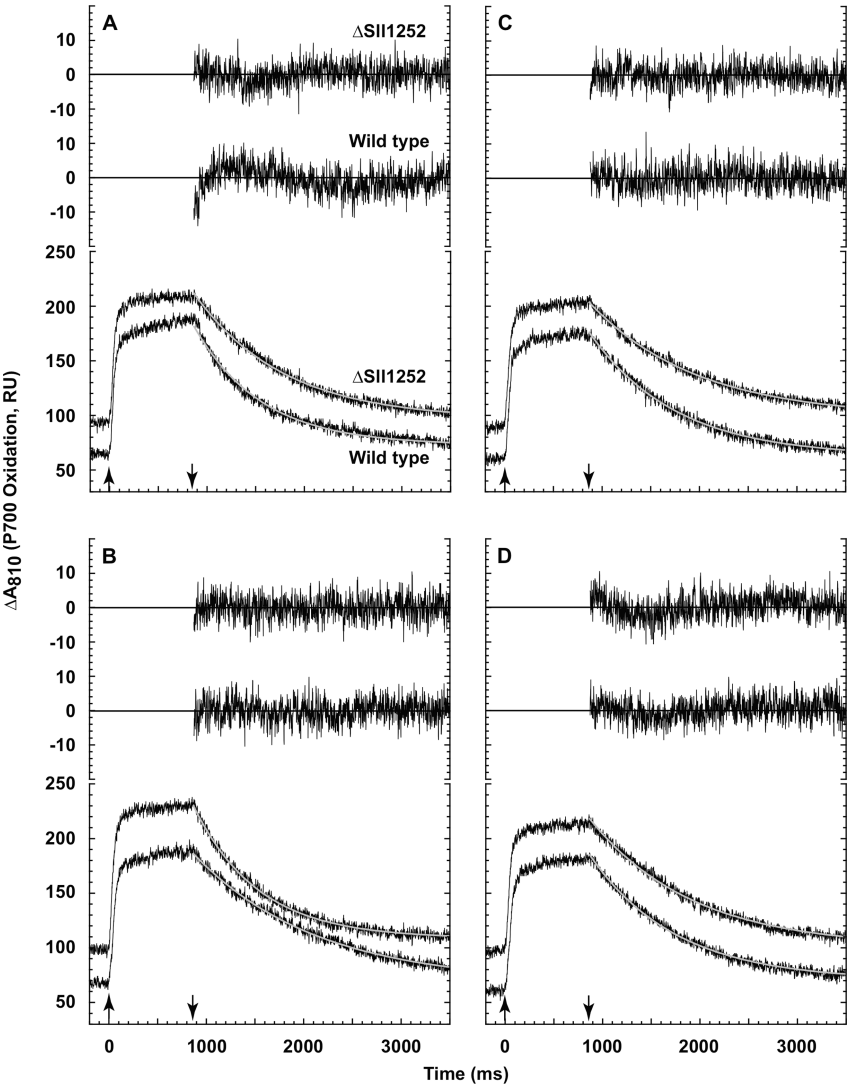

FIGURE 6: Activity of cyclic electron flow assessed by the light-induced oxidation−reduction kinetics of P700. (A−D) The absorbance changes of P700 at 810 nm were recorded using a PAM101 fluorometer equipped with a dual-wavelength P700 unit (ED-P700DW) in the presence of 50 μM DCMU at a concentration of 4 μg of Chl/mL: (bottom lines) wild-type cells and (top lines) ΔSll1252 cells. (A) Cells grown in normal BG11 medium. (B) Cells grown in Ca^{2+}-depleted medium. (C) Cells grown in Cl^--depleted medium. (D) Cells grown in Ca^{2+}- and Cl^--depleted medium. Actinic light was turned on and off at the times indicated by the arrows (upward, turn on; downward, turn off). Typical traces are shown along with fitting curves for the re-reduction kinetics after the light had been turned off. Curve fitting was performed using KaleidaGraph with a Levenberg−Marquardt regression algorithm. The curves were better fitted with one exponential decay component. Residuals are presented atop each panel.

electrophoresis (Figure 9). The Chl-specific amounts of heme associated with cytochrome *f* were comparable between wild-type and ΔSll1252 cells grown in normal BG11 medium. When the cells were grown in the Ca^{2+}- and Cl^--depleted medium, the level of cytochrome *f*-associated heme increased remarkably in wild-type cells. The Chl-specific amount of PsbA/B was almost the same irrespective of the strains and growth conditions, although a slight decrease seemed to occur in wild-type cells grown in the Ca^{2+}- and Cl^--depleted medium. The Chl-specific amounts of PS II polypeptides (PsbC, PsbO, and cytochrome c_{550}) seemed to be slightly increased in wild-type cells grown in the Ca^{2+}- and Cl^--depleted medium, and they were slightly decreased in the mutant cells grown in normal BG11 compared with wild-type cells and, especially cyt c_{500}, were more decreased when they were grown in the Ca^{2+}- and Cl^--depleted medium (Figure 9). The level of IsiA was increased in the mutant cells especially when they were grown in the Ca^{2+}- and Cl^--depleted medium. In PS II complexes purified from mutant cells (ΔSll1252/HT3) grown in normal BG11

Table 3: Half-Times of P700 Re-Reduction via Cyclic Electron Flow, Plastocyanin/Cytochrome c_6, or Cytochrome b_6/f[a]

		half-decay time (ms)			
route to re-reduce P700	strain	BG11	without Ca^{2+}	without Cl^-	without Ca^{2+} and Cl^-
cyclic electron flow	wild-type	440 ± 84	830 ± 21	620 ± 12	650 ± 23
	ΔSll1252	580 ± 31	510 ± 29	820 ± 40	760 ± 26
plastocyanin/cytochrome c_6	wild-type	160 ± 17	200 ± 5.6	110 ± 1.3	66 ± 0.43
	ΔSll1252	180 ± 2.5	130 ± 1.3	64 ± 5.7	55 ± 0.75
cytochrome b_6/f	wild-type	110 ± 15	130 ± 12	730 ± 140	1200 ± 56
	ΔSll1252	330 ± 50	240 ± 16	2100 ± 40	2000 ± 100

[a]The decay curves after illumination as shown in Figures 6 (50 μM DCMU), 7 (1 mM sodium ascorbate and 0.1 mM DCIP as electron donors for plastocyanin/cytochrome c_6, and 50 μM DCMU), and 8 (5 mM sodium ascorbate and 0.5 mM duroquinone as electron donors to cytochrome b_6/f, and 50 μM DCMU) for the measurements of P700 re-reduction via cyclic electron flow, plastocyanin/cytochrome c_6, and cytochrome b_6/f, respectively, and fitted using KaleidaGraph with a Levenberg−Marquardt regression algorithm. The curves were fitted with one exponential decay component. SE values are given (n = 3).

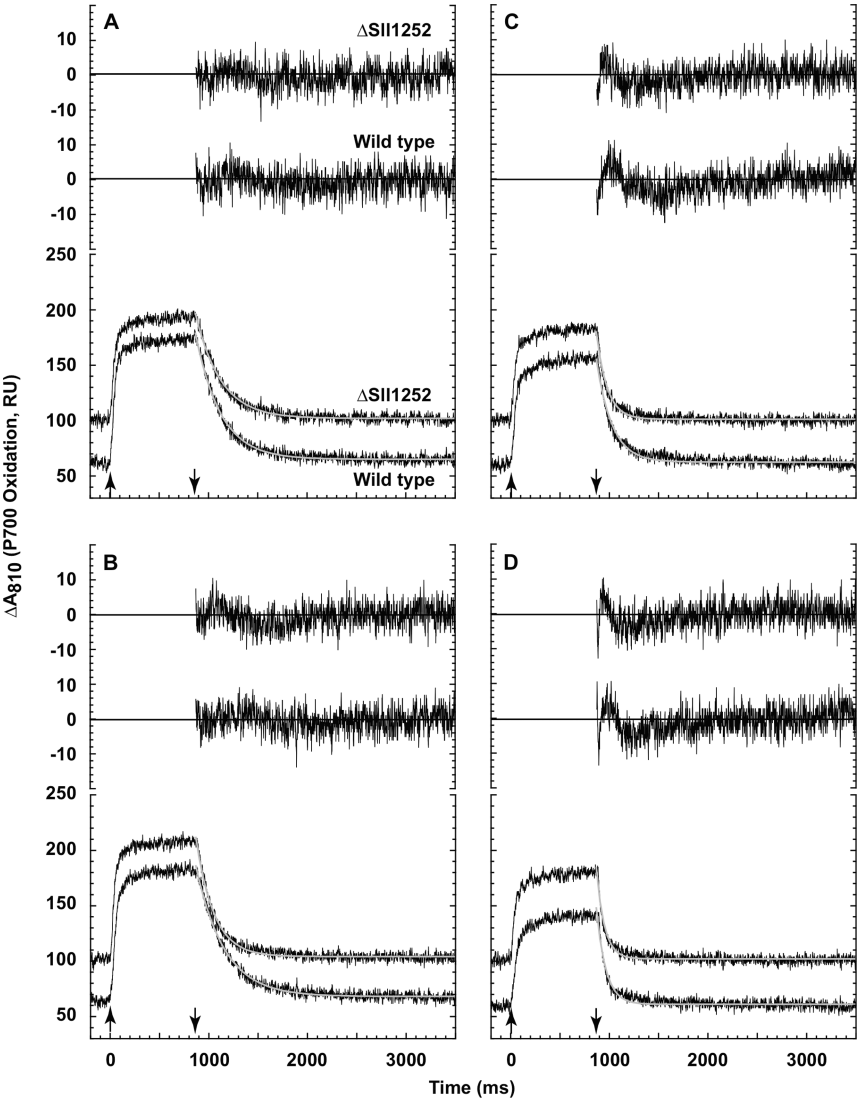

FIGURE 7: Electron donation via plastocyanin/cytochrome c_6 to P700 assessed by the light-induced oxidation−reduction kinetics of P700. (A−D) The absorbance changes of P700 at 810 nm were recorded using a PAM101 fluorometer equipped with a dual-wavelength P700 unit (ED-P700DW) in the presence of 1 mM sodium ascorbate and 0.1 mM DCIP as electron donors for plastocyanin and 50 μM DCMU at a concentration of 4 μg of Chl/mL: (bottom lines) wild-type cells and (top lines) ΔSll1252 cells. (A) Cells grown in normal BG11 medium. (B) Cells grown in Ca^{2+}-depleted medium. (C) Cells grown in Cl^--depleted medium. (D) Cells grown in Ca^{2+}- and Cl^--depleted medium. Actinic light was turned on and off at the times indicated by the arrows (upward, turn on; downward, turn off). Typical traces are shown along with fitting curves for the re-reduction kinetics after the light had been turned off. The curves were fitted with one exponential decay component. Residuals are presented atop each panel.

medium, the amounts of cytochrome c_{550} (PsbV) and other extrinsic proteins (PsbO, PsbQ, and PsbU) were decreased (Figure S4 of the Supporting Information, lane 4). The decrease in the level of cytochrome c_{550} was further verified by means of chemical titration in PS II complexes purified from wild-type (HT3) and mutant (ΔSll1252/HT3) cells (data not shown).

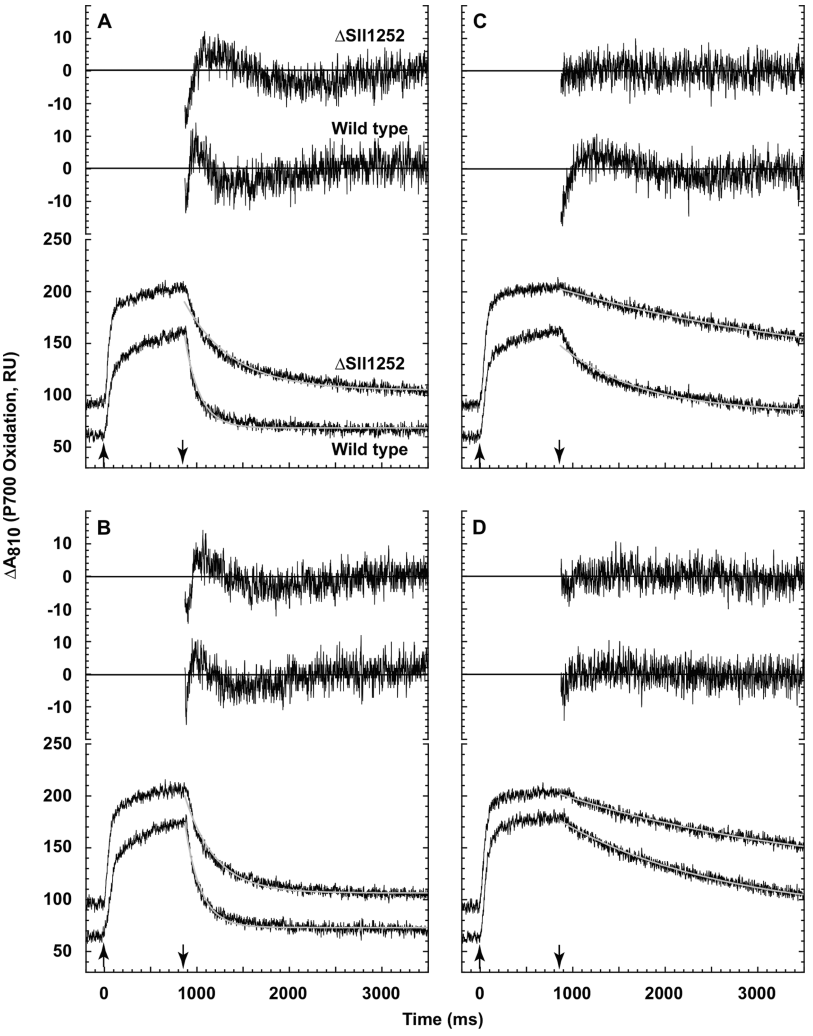

FIGURE 8: Electron donation activity via cytochrome b_6/f to P700 assessed by the light-induced oxidation−reduction kinetics of P700. (A−D) The absorbance changes of P700 were recorded at 810 nm using a PAM101 fluorometer equipped with a dual-wavelength P700 unit (ED-P700DW) in the presence of 5 mM sodium ascorbate and 0.5 mM duroquinone as electron donors for cytochrome b_6/f and 50 μM DCMU at a concentration of 4 μg of Chl/mL: (bottom lines) wild-type cells and (top lines) ΔSll1252 cells. (A) Cells grown in normal BG11 medium. (B) Cells grown in Ca^{2+}-depleted medium. (C) Cells grown in Cl^--depleted medium. (D) Cells grown in Ca^{2+}- and Cl^--depleted medium. Actinic light was turned on and off at the times indicated by the arrows (upward, turn on; downward, turn off). Typical traces are shown along with fitting curves for the re-reduction kinetics after the light had been turned off. The curves were fitted with one exponential decay component. Residuals are presented atop each panel.

DISCUSSION

Because the shape and size of ΔSll1252 cells were not altered under our growth conditions, it is highly likely that Sll1252 functions separately from the cell division machinery. The expression level of Sll1252 was considerably low (data not shown). Despite the failure to detect Sll1252 tightly associated with PS II, genetic deletion of *sll1252* resulted in functional disorders in the PS II machinery, especially when the cells were grown in medium depleted of Cl^- ions that are necessary for the functional machinery for water oxidation in PS II (*21*, *44*, *45*) (Figure S2 and Tables S1 and S2 of the Supporting Information). These apparent functional impairments could be attributed to the extended vulnerability of the PS II core complexes in ΔSll1252 cells upon depletion of Cl^- from the growth medium (Figure S4 of the Supporting Information).

These findings support the idea that the Sll1252 protein is involved in the functional machinery of PS II. However, the absence of Sll1252 showed global effects on the photosynthetic function beyond the involvement of PS II. The reduction level of Q_A, and consequently that of the plastoquinone pool, increased in ΔSll1252 cells. Despite the greater level of reduction of Q_A during illumination with actinic light, P700 was more oxidized in ΔSll1252 cells than in wild-type cells (Table 2). The electron donation rate itself through plastocyanin/cytochrome c_6 from an artificial electron donor (reduced DCIP) was not altered (Figure 7 and Table 3), while the electron donation rates through cytochrome b_6/f were greatly decelerated (Figure 8 and Table 3) in ΔSll1252 cells under all the growth conditions tested. These results clearly indicate that functional impairments have occurred in the electron flow in cytochrome b_6/f complexes following deletion of Sll1252. The dysfunction of cytochrome b_6/f complexes can explain the more oxidized state of P700 during light illumination (Figure 5 and Table 2). The heme staining analysis suggested assembly failure of cytochriome b_6/f complexes (Figure 9).

Some of the results obtained in this study, such as those shown in Figures 2 and 4 and Table 1, can be ascribed to the more greatly reduced levels of the cellular inner environments in ΔSll1252 cells, i.e., indirect effects on PS II resulting from altered redox poising leading to greater photoinhibition. The more reduced plastoquinone pool could result from dysfunction of

the respiratory chain, which shares plastoquinones and cytochrome b_6/f complexes as electron carriers (*46*), if Sll1252 participates in the function of the respiratory chain rather than the photosynthetic electron transport chain. However, considering the localization of the homologous protein in *Arabidopsis* chloroplasts, it is more reasonable that Sll1252 functions in the photosynthesis-related machinery rather than in the respiratory-related machinery. Additionally, very similar results were reported for the PsbP-knockdown mutant of higher plants: increase in the proportion of reduced Q_A and oxidized P700 under the light and the slow fluorescence quenching after the saturation pulse in the dark (*47*−*49*).

It seems that cells lacking Sll1252 have increased sensitivity to Cl^- depletion. Rather, we prefer the idea that ΔSll1252 cells perceive stress to be greater than it was. For example, IsiA, which is expressed under stress conditions (*42*), was even present in Sll1252 cells grown in normal BG11 medium (Figure 3A,D), and the level of IsiA increased much more when the cells were grown in the Cl^--depleted medium (Figure 3B,E). The profile of the transient fluorescence increase after a saturating flash in the dark observed in ΔSll1252 cells grown in normal BG11 medium was almost identical to that observed in wild-type cells grown in the Cl^--depleted medium (compare panels B and C of Figure 4). The re-reduction kinetics of P700 via cytochrome b_6/f complexes in ΔSll1252 cells grown in normal BG11 medium were similar to those in wild-type cells grown in the Ca^{2+}- or Cl^--depleted medium (Figure 8A−C). Hence, Sll1252 is closely related to the machinery involved in coping with environmental stress. These profiles are consistent with the recent findings through global proteomics that the expression level of Sll1252 is elevated after release from various kinds of nutrient starvation (Fe, N, or S) (*50*). Furthermore, an interaction of Sll1252 with Sll1003 was observed by yeast two-hybrid assays (*51*). Sll1003 is a two-component sensor histidine kinase that is assumed to be essential for growth (*52*). In this context, it is more reasonable to consider that Sll1252 functions in a global cellular system required to cope with environmental stress (Figure 10) rather than being restricted to the regulation of PS II alone.

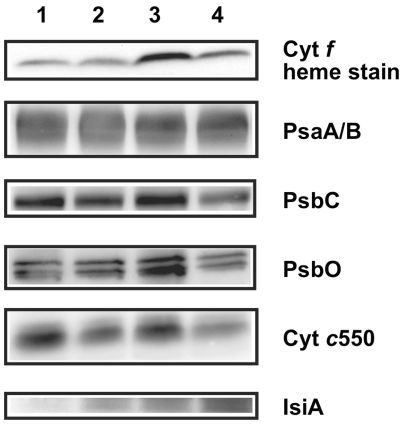

FIGURE 9: Polypeptides of electron transport complexes in cells grown in normal or Ca^{2+}- and Cl^--depleted BG11 medium: lane 1, wild-type cells grown in normal BG11 medium; lane 2, ΔSll1252 cells grown in normal BG11 medium; lane 3, wild-type cells grown in Ca^{2+}- and Cl^--depleted medium; lane 4, ΔSll1252 cells grown in Ca^{2+}- and Cl^--depleted medium. Cytochrome *f* was visualized by heme staining, and others were visualized using specific antibodies. Samples corresponding to 7 or 1.3 μg of Chl were applied for heme staining or immunodetection, respectively.

In our working model presented in Figure 10, the reducing state of the plastoquinone pool caused by environmental stress would be detected by currently unknown signal sensors that lead to the activation of Sll1252 in the wild type (Figure 10A). One of the plausible signal sensors is Hik13 (*51*). The S4 domain of Sll1252 could be involved in the activation. Activated Sll1252 may participate in the regulation of the amounts of proteins and/or enzymes related to photosynthetic electron flow, such as cytochrome *f* and cytochrome c_{550}, to balance the redox status of the electron transport system. Because the electron flow through cytochrome b_6/f complexes was decelerated (Figure 8 and Table 3) and the PS II-mediated Hill reaction with 2,5-DCBQ as an electron acceptor was affected (Figure S2 and Table S1 of the Supporting Information) by the absence of Sll1252, Sll1252 may participate in the structural and/or functional assembly of these complexes. Under severe stress that induces a very high reducing state, another route for the sensory cascade

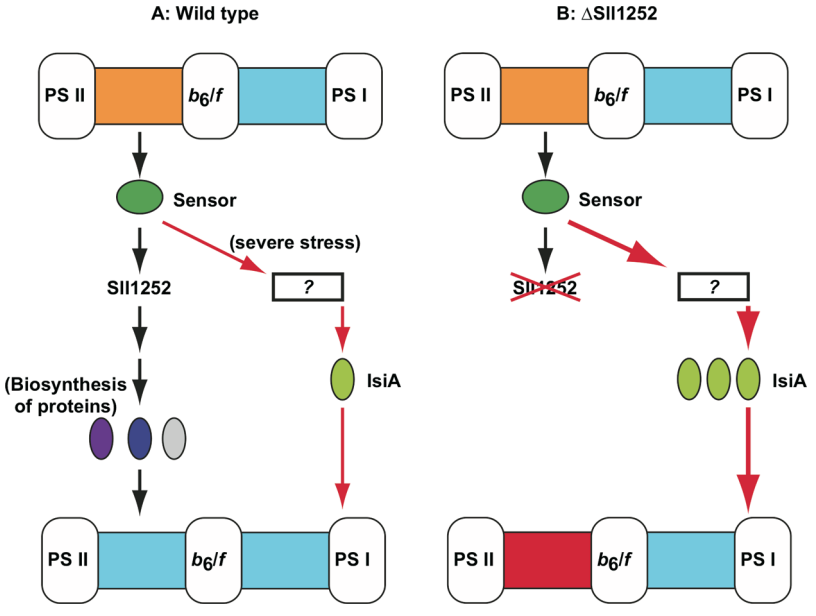

FIGURE 10: Schematic working model of the function of Sll1252. The reducing levels of thylakoids are expressed in different colors, with warmer colors indicating higher reducing levels. See the text for details.

would work to suppress the amounts of PS I and PS II and induce a large amount of IsiA.

In the absence of Sll1252 (Figure 10B), the regulation system through Sll1252 would be disordered and dysfunction of cytochrome b_6/f complexes as well as PS II would occur, consequently leading to a higher reducing status of the plastoquinone pool even under the normal growth conditions (Figure 4). Environmental stress such as Cl^- depletion would easily cause a high reducing level of plastoquinone without Sll1252, and a higher reducing level of the plastoquinone pool would result in the induction of IsiA production (Figure 10B).

Therefore, we can conclude that Sll1252 is involved in the signal transduction cascade required to cope with environmental stress to achieve a redox balance of the photosynthetic electron transport system. Furthermore, taking into account that Sll1252 has an S4 domain, we find it is possible that Sll1252 participates in the assembly process of cytochromes and/or other subunit components for both PS II and cytochrome b_6/f complexes to make them functional forms.

ACKNOWLEDGMENT

We thank Dr. Terry M. Bricker for the HT3 cells and Drs. Toshiharu Hase and Hirozo Oh-oka for valuable discussions.

SUPPORTING INFORMATION AVAILABLE

Figures S1−S4 and Tables S1 and S2. This material is available free of charge via the Internet at http://pubs.acs.org.

REFERENCES

1. Ferreira, K. N., Iverson, T. M., Maghlaoui, K., Barber, J., and Iwata, S. (2004) Architecture of the photosynthetic oxygen-evolving center. *Science 303*, 1831–1838.
2. Guskov, A., Kern, J., Gabdulkhakov, A., Broser, M., Zouni, A., and Saenger, W. (2009) Cyanobacterial photosystem II at 2.9-Å resolution and the role of quinones, lipids, channels and chloride. *Nat. Struct. Mol. Biol. 16*, 334–342.
3. Kamiya, N., and Shen, J.-R. (2003) Crystal structure of oxygen-evolving photosystem II from *Thermosynechococcus vulcanus* at 3.7-Å resolution. *Proc. Natl. Acad. Sci. U.S.A. 100*, 98–103.
4. Loll, B., Kern, J., Saenger, W., Zouni, A., and Biesiadka, J. (2005) Towards complete cofactor arrangement in the 3.0 Å resolution structure of photosystem II. *Nature 438*, 1040–1044.
5. Kashino, Y., Lauber, W. M., Carroll, J. A., Wang, Q., Whitmarsh, J., Satoh, K., and Pakrasi, H. B. (2002) Proteomic analysis of a highly active photosystem II preparation from the cyanobacterium *Synechocystis* sp. PCC 6803 reveals the presence of novel polypeptides. *Biochemistry 41*, 8004–8012.
6. Kashino, Y., Inoue-Kashino, N., Roose, J. L., and Pakrasi, H. B. (2006) Absence of the PsbQ protein results in destabilization of the PsbV protein and decreased oxygen evolution activity in cyanobacterial photosystem II. *J. Biol. Chem. 281*, 20834–20841.
7. Thornton, L. E., Ohkawa, H., Roose, J. L., Kashino, Y., Keren, N., and Pakrasi, H. B. (2004) Homologs of plant PsbP and PsbQ proteins are necessary for regulation of photosystem II activity in the cyanobacterium, *Synechocystis* 6803. *Plant Cell 16*, 2164–2175.
8. Keren, N., Ohkawa, H., Welsh, E. A., Liberton, M., and Pakrasi, H. B. (2005) Psb29, a conserved 22-kD protein, functions in the biogenesis of Photosystem II complexes in *Synechocystis* and *Arabidopsis*. *Plant Cell 17*, 2768–2781.
9. Sirpio, S., Allahverdiyeva, Y., Suorsa, M., Paakkarinen, V., Vainonen, J., Battchikova, N., and Aro, E. M. (2007) TLP18.3, a novel thylakoid lumen protein regulating photosystem II repair cycle. *Biochem. J. 406*, 415–425.
10. Chen, H., Zhang, D., Guo, J., Wu, H., Jin, M., Lu, Q., Lu, C., and Zhang, L. (2006) A Psb27 homologue in *Arabidopsis thaliana* is required for efficient repair of photodamaged photosystem II. *Plant Mol. Biol. 61*, 567–575.
11. Nowaczyk, M. M., Hebeler, R., Schlodder, E., Meyer, H. E., Warscheid, B., and Rogner, M. (2006) Psb27, a cyanobacterial lipoprotein, is involved in the repair cycle of photosystem II. *Plant Cell 18*, 3121–3131.
12. Roose, J. L., and Pakrasi, H. B. (2008) The Psb27 protein facilitates manganese cluster assembly in photosystem II. *J. Biol. Chem. 283*, 4044–4050.
13. Aravind, L., and Koonin, E. V. (1999) Novel predicted RNA-binding domains associated with the translation machinery. *J. Mol. Evol. 48*, 291–302.
14. Davies, C., Gerstner, R. B., Draper, D. E., Ramakrishnan, V., and White, S. W. (1998) The crystal structure of ribosomal protein S4 reveals a two-domain molecule with an extensive RNA-binding surface: One domain shows structural homology to the ETS DNA-binding motif. *EMBO J. 17*, 4545–4558.
15. Fadda, D., Pischedda, C., Caldara, F., Whalen, M. B., Anderluzzi, D., Domenici, E., and Massidda, O. (2003) Characterization of *divIVA* and other genes located in the chromosomal region downstream of the *dcw* cluster in *Streptococcus pneumoniae*. *J. Bacteriol. 185*, 6209–6214.
16. Finn, R. D., Mistry, J., Tate, J., Coggill, P., Heger, A., Pollington, J. E., Gavin, O. L., Gunasekaran, P., Ceric, G., Forslund, K., Holm, L., Sonnhammer, E. L. L., Eddy, S. R., and Bateman, A. (2010) The Pfam protein families database. *Nucleic Acids Res. 38*, D211–D222.
17. Miyagishima, S. Y., Wolk, C. P., and Osteryoung, K. W. (2005) Identification of cyanobacterial cell division genes by comparative and mutational analyses. *Mol. Microbiol. 56*, 126–143.
18. Hoiczyk, E., and Hansel, A. (2000) Cyanobacterial cell walls: News from an unusual prokaryotic envelope. *J. Bacteriol. 182*, 1191–1199.
19. Emanuelsson, O., Brunak, S., von Heijne, G., and Nielsen, H. (2007) Locating proteins in the cell using TargetP, SignalP and related tools. *Nat. Protoc. 2*, 953–971.
20. Zybailov, B., Rutschow, H., Friso, G., Rudella, A., Emanuelsson, O., Sun, Q., and van Wijk, K. J. (2008) Sorting signals, N-terminal modifications and abundance of the chloroplast proteome. *PLoS One 3*, e1994.
21. Inoue-Kashino, N., Kashino, Y., Satoh, K., Terashima, I., and Pakrasi, H. B. (2005) PsbU provides a stable architecture for the oxygen-evolving system in cyanobacterial photosystem II. *Biochemistry 44*, 12214–12228.
22. Stanier, R. Y., Kunisawa, R., Mandel, M., and Cohen-Bazire, G. (1971) Purification and properties of unicellular blue-green algae (order *Chroococcales*). *Bacteriol. Rev. 35*, 171–205.
23. Kaneko, T., Sato, S., Kotani, H., Tanaka, A., Asamizu, E., Nakamura, Y., Miyajima, N., Hirosawa, M., Sugiura, M., Sasamoto, S., Kimura, T., Hosouchi, T., Matsuno, A., Muraki, A., Nakazaki, N., Naruo, K., Okumura, S., Shimpo, S., Takeuchi, C., Wada, T., Watanabe, A., Yamada, M., Yasuda, M., and Tabata, S. (1996) Sequence analysis of the genome of the unicellular cyanobacterium *Synechocystis* sp. strain PCC 6803. II. Sequence determination of the entire genome and assignment of potential protein-coding regions. *DNA Res. 3*, 109–136.
24. Schweizer, H. D. (1993) Small broad-host-range gentamycin resistance gene cassettes for site-specific insertion and deletion mutagenesis. *BioTechniques 15*, 831–834.
25. Bricker, T. M., Morvant, J., Masri, N., Sutton, H. M., and Frankel, L. K. (1998) Isolation of a highly active photosystem II preparation from *Synechocystis* 6803 using a histidine-tagged mutant of CP 47. *Biochim. Biophys. Acta 1409*, 50–57.
26. Oka, A., Sugisaki, H., and Takanami, M. (1981) Nucleotide sequence of the kanamycin resistance transposon Tn*903*. *J. Mol. Biol. 147*, 217–226.
27. Inoue-Kashino, N., Takahashi, T., Ban, A., Sugiura, M., Takahashi, Y., Satoh, K., and Kashino, Y. (2008) Evidence for a stable association of Psb30 (Ycf12) with photosystem II core complex in the cyanobacterium *Synechocystis* sp. PCC 6803. *Photosynth. Res. 98*, 323–335.
28. Kashino, Y. (2003) Separation methods in the analysis of protein membrane complexes. *J. Chromatogr., B 797*, 191–216.
29. Kashino, Y., Koike, H., and Satoh, K. (2001) An improved sodium dodecyl sulfate-polyacrylamide gel electrophoresis system for the analysis of membrane protein complexes. *Electrophoresis 22*, 1004–1007.
30. Kashino, Y., Enami, I., Satoh, K., and Katoh, S. (1990) Immunological cross-reactivity among corresponding proteins of photosystems I and II from widely divergent photosynthetic organisms. *Plant Cell Physiol. 31*, 479–488.
31. Enami, I., Iwai, M., Akiyama, A., Suzuki, T., Okumura, A., Katoh, T., Tada, O., Ohta, H., and Shen, J. R. (2003) Comparison of binding and functional properties of two extrinsic components, Cyt c550 and a 12 kDa protein, in cyanobacterial PSII with those in red algal PSII. *Plant Cell Physiol. 44*, 820–827.
32. Porra, R. J., Thompson, W. A., and Kriedemann, P. E. (1989) Determination of accurate extinction coefficients and simultaneous equations for assaying chlorophylls *a* and *b* extracted with four different solvents: Verification of the concentration of chlorophyll

standards by atomic absorption spectroscopy. *Biochim. Biophys. Acta 975*, 384–394.
33. Eilers, P. H. C., and Peeters, J. C. H. (1988) A model for the relationship between light intensity and the rate of photosynthesis in phytoplankton. *Ecol. Modell. 42*, 199–215.
34. Meetam, M., Keren, N., Ohad, I., and Pakrasi, H. B. (1999) The PsbY protein is not essential for oxygenic photosynthesis in the cyanobacterium *Synechocystis* sp. PCC 6803. *Plant Physiol. 121*, 1267–1272.
35. Fujimori, T., Hihara, Y., and Sonoike, K. (2005) PsaK2 subunit in photosystem I is involved in state transition under high light condition in the cyanobacterium *Synechocystis* sp. PCC 6803. *J. Biol. Chem. 280*, 22191–22197.
36. Kyte, J., and Doolittle, R. F. (1982) A simple method for displaying the hydropathic character of a protein. *J. Mol. Biol. 157*, 105–132.
37. Hirokawa, T., Boon-Chieng, S., and Mitaku, S. (1998) SOSUI: Classification and secondary structure prediction system for membrane proteins. *Bioinformatics 14*, 378–379.
38. Gasteiger, E., Hoogland, C., Gattiker, A., Duvaud, S., Wilkins, M. R., Appel, R. D., and Bairoch, A. (2005) Protein Identification and Analysis Tools on the ExPASy Server. In The Proteomics Protocols Handbook (Walker, J. M., Ed.) pp 571−607, Humana Press, Totowa, NJ.
39. Juncker, A. S., Willenbrock, H., Von Heijne, G., Brunak, S., Nielsen, H., and Krogh, A. (2003) Prediction of lipoprotein signal peptides in Gram-negative bacteria. *Protein Sci. 12*, 1652–1662.
40. Emanuelsson, O., Nielsen, H., and von Heijne, G. (1999) ChloroP, a neural network-based method for predicting chloroplast transit peptides and their cleavage sites. *Protein Sci. 8*, 978–984.
41. Burnap, R. L., Troyan, T., and Sherman, L. A. (1993) The highly abundant chlorophyll-protein complex of iron-deficient *Synechococcus* sp. PCC7942 (CP43′) is encoded by the *isiA* gene. *Plant Physiol. 103*, 893–902.
42. Shcolnick, S., Summerfield, T. C., Reytman, L., Sherman, L. A., and Keren, N. (2009) The mechanism of iron homeostasis in the unicellular cyanobacterium *Synechocystis* sp. PCC 6803 and its relationship to oxidative stress. *Plant Physiol. 150*, 2045–2056.
43. Morand, L. Z., Cheng, R. H., Krogmann, D. W., and Ho, K. K. (1994) Soluble Electron Transfer Catalysts of Cyanobacteria. In The Molecular Biology of Cyanobacteria (Bryant, D. A., Ed.) pp 381−407, Kluwer Academic Publishers, Dordrecht, The Netherlands.
44. Bricker, T. M., Young, A., Frankel, L. K., and Putnam-Evans, C. (2002) Introduction of the 305Arg→305Ser mutation in the large extrinsic loop E of the CP43 protein of *Synechocystis* sp. PCC 6803 leads to the loss of cytochrome c_{550} binding to Photosystem II. *Biochim. Biophys. Acta 1556*, 92–96.
45. Itoh, S., and Uwano, S. (1986) Characteristics of the Cl^- action site in the O_2 evolving reaction in PS II particles: Electrostatic interaction with ions. *Plant Cell Physiol. 27*, 25–36.
46. Schmetterer, G. (1994) Cyanobacterial Respiration. In The Molecular Biology of Cyanobacteria (Bryant, D. A., Ed.) pp 409−435, Kluwer Academic Publishers, Dordrecht, The Netherlands.
47. Ido, K., Ifuku, K., Yamamoto, Y., Ishihara, S., Murakami, A., Takabe, K., Miyake, C., and Sato, F. (2009) Knockdown of the PsbP protein does not prevent assembly of the dimeric PSII core complex but impairs accumulation of photosystem II supercomplexes in tobacco. *Biochim. Biophys. Acta 1787*, 873–881.
48. Ifuku, K., Yamamoto, Y., Ono, T. A., Ishihara, S., and Sato, F. (2005) PsbP protein, but not PsbQ protein, is essential for the regulation and stabilization of photosystem II in higher plants. *Plant Physiol. 139*, 1175–1184.
49. Yi, X., Hargett, S. R., Liu, H., Frankel, L. K., and Bricker, T. M. (2007) The PsbP protein is required for photosystem II complex assembly/stability and photoautotrophy in *Arabidopsis thaliana*. *J. Biol. Chem. 282*, 24833–24841.
50. Wegener, K. M., Singh, A. K., Jacobs, J. M., Elvitigala, T. R., Welsh, E. A., Keren, N., Gritsenko, M. A., Ghosh, B. K., Camp, D. G., Smith, R. D., and Pakrasi, H. B. (2010) Global proteomics reveal an atypical strategy for carbon/nitrogen assimilation by a cyanobacterium under diverse environmental perturbations. *Mol. Cell. Proteomics* (in press).
51. Sato, S., Shimoda, Y., Muraki, A., Kohara, M., Nakamura, Y., and Tabata, S. (2007) A large-scale protein protein interaction analysis in *Synechocystis* sp. PCC6803. *DNA Res. 14*, 207–216.
52. Suzuki, I., Los, D. A., Kanesaki, Y., Mikami, K., and Murata, N. (2000) The pathway for perception and transduction of low-temperature signals in *Synechocystis*. *EMBO J. 19*, 1327–1334.